Journal of Constructional Steel Research 73 (2012) 43–54

Contents lists available at SciVerse ScienceDirect

Journal of Constructional Steel Research

Elastic rigidity of composite beams with full width slab openings

Jian-Guo Nie [a], Yu-Hang Wang [a,*], C.S. Cai [b]

[a] Key Laboratory of Structural Engineering and Vibration of China Education Ministry, Dept. of Civil Engineering, Tsinghua University, Beijing 100084, China
[b] Department of Civil and Environmental Engineering, Louisiana State University, Baton Rouge, LA 70803, USA

ARTICLE INFO

Article history:
Received 18 October 2011
Accepted 24 January 2012
Available online 6 March 2012

Keywords:
Steel-concrete
Composite beam
Full openings
Elastic rigidity

ABSTRACT

Openings often exist in the concrete slab of composite floors due to the functional requirements of structures. The strength and rigidity of steel-concrete composite beams are reduced by openings. Based on three tests of steel-concrete composite beams with full openings in the concrete flange, the elastic rigidity of composite beams is analyzed. Finite element analysis (FEA) considering the slip effect between the steel and concrete is conducted to simulate the composite beams with full openings in the concrete slab, and the results show that the FEA method is reliable. The analytical calculation method for the deflection of composite beams with full openings in the concrete slab is also proposed, and the results are verified by tests. The predicted deflections using the analytical method and FEA method both agree well with the test results. It is further verified that openings near the supports have insignificant effects on the deflection at the mid-span and this effect can be thus ignored. The simplified method to calculate the rigidity reduction factor is developed by a regression analysis. The analytical method and FEA method can be used for the serviceability limit state design of steel-concrete composite beams with full openings in the concrete flange.

1. Introduction

Steel-concrete composite floors are widely used in buildings [1]. Compared with conventional reinforced concrete floors, steel-concrete composite floors have major advantages in their bending resistance and stiffness by fully utilizing the material strength of both steel and concrete, and taking advantage of light weight and rapid construction features.

Often in order to satisfy functional requirements such as placing heating, ventilating, and water pipes and electric wires, the floors have to be cast with openings. Large openings are also required in industrial buildings. From Fig. 1(a) it can be seen that openings even exist directly over the flanges of steel beams, which are called full openings. When there are openings in the floor, the concrete flange of steel-concrete composite beam is weakened and a stress concentration occurs at the openings, which might significantly affect the flexural strength and rigidity of structures. If the composite effects between the concrete slab and steel beam are not considered in design, i.e., ignoring the composite action, construction cost will be increased due to this conservatism. Therefore, it is necessary to consider the composite action and effects of openings on the rigidity of steel-concrete composite beams.

Refs. [2–4] studied the composite beams with web openings and described the procedures for calculating the shear capacity and deflections of beams. Ref. [5] studied the rigidity and flexural strength of composite beams with opening rate below 50%, as shown in Fig. 1(b). The opening rate was defined as the ratio of the area of the cross section with openings and the section without openings in the concrete flange. Research on the rigidity and flexural strength of steel-concrete composite beams with full openings (a 100% opening rate) in the concrete flange was not reported in the literature.

The concrete slab of composite beams with full openings is divided into several independent parts by the full openings, and the compressive stress flow in the concrete flange is interrupted and not continuous. Therefore, the rigidity and flexural strength of composite beams with full openings in concrete slab are much different from those with opening rates below 50%. Based on experimental observations, in the present study, the FEA method and theoretical method were both developed to calculate the elastic rigidity of composite beams with full openings in the concrete slab. The effects of openings and slip between the concrete slab and steel beam on the elastic rigidity were both considered in the FEA method and theoretical method.

2. Experimental study

2.1. Specimens

Three specimens were tested to study the mechanical behavior of steel-concrete composite beams with full openings in the concrete flange under static load by changing the position of openings. The three test specimens were designed based on ref. [5], and were identified as KCB4-1, KCB4-2 and KCB4-3. The full openings were located

* Corresponding author.
E-mail address: wangyh04@mails.tsinghua.edu.cn (Y.-H. Wang).

0143-974X/$ – see front matter © 2012 Elsevier Ltd. All rights reserved.
doi:10.1016/j.jcsr.2012.01.008

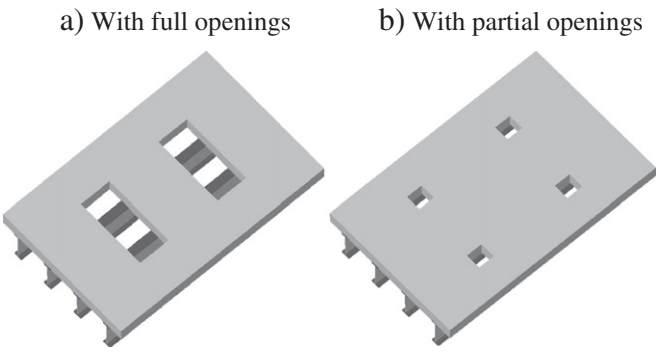

Fig. 1. Steel-concrete composite floor with openings in slab.

at the mid-span, 950 mm from the mid-span, and near the support, and named type 1, type 2, and type 3 openings, respectively. The 3.9 m long beams had 800 mm wide by 110 mm thick cast-in-place concrete slab fully connected to a 200×100 I-section steel beam. Shear studs of 16-mm diameter by 90 mm long were welded in line to the top flange of the steel beam, at a spacing of 120 mm. The measured mean compressive strength of the concrete was $f_{cu}=32.3$ MPa, and the steel used for the I-section beams had a mean tensile yield strength f_y of 325 MPa. The ultimate strength of the studs used in the specimens was 406 MPa. The main physical dimensions of the three specimens were shown in Fig. 2.

2.2. Instrumentation

All the specimens were simply supported, loaded in two points symmetrical about the mid-span, having a space of 1100 mm between the loading points. The load was transferred through a series of spreader beams to the top flange of concrete slab. The specimens were statically loaded and the loading scheme is shown in Fig. 3.

2.3. Experimental results

According to the tests, the initial plane sections of composite beams with openings remained plane when loaded. With the increase of load, the curvature of the composite section increased and the neutral axis moved upwards. When the top of the concrete flange reached the limiting strain, the composite beam reached to the flexural strength. All the specimens were designed with full shear connections. There were no observed longitudinal splitting cracks in the concrete slab during the tests.

The mechanical behavior of the three specimens was nearly the same before the steel section yielded. The concrete slab and steel beam worked together well. There were no cracks in the concrete slab because the neutral axis was located within the steel beam

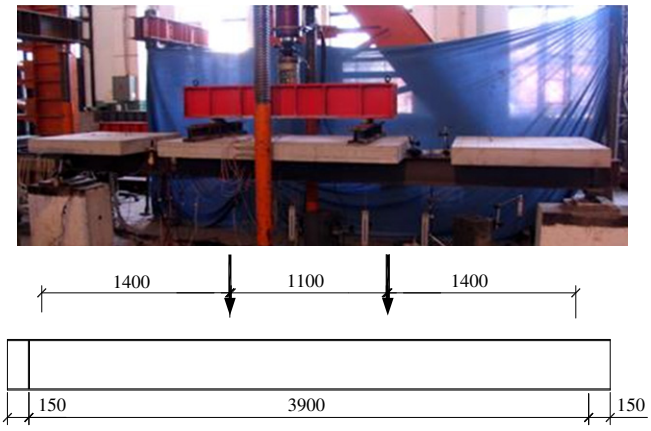

Fig. 3. Loading scheme of beam tests (unit = mm).

section. As shown in Fig. 4, the load–deflection curves approaches to a straight line in the elastic stage. The aim of this paper was to present the elastic method for calculating the deflection of steel-concrete composite beams with full openings in the concrete flange. The main experimental results were shown in Table 1.

The specimen KCB4-1 underwent elastic, elastic–plastic and descending stages. The steel beam without a concrete slab at mid-span was the weakest segment and lateral torsional movement occurred at the ultimate state. Cracks appeared on the bottom of the concrete slab of specimen KCB4-2 when it was loaded up to 118 kN (0.98 P_u), then lateral torsional failure happened. The specimen KCB4-3 also underwent elastic, elastic–plastic and descending stages. The flexural strength and rigidity were higher than that of KCB4-1 and KCB4-2. When the load was up to 174 kN, cracks appeared on the bottom of the concrete slab obviously. The elastic–plastic stage was long, and the ductility was good for this specimen with a ductility factor of 11.0. The ductility factor was defined as the ratio of the ultimate displacement to the yielding displacement at the mid-span. Finally the concrete at the shear span crushed when the load reached 248 kN.

The relationships between load and steel strain at the bottom of the steel beam were given in Fig. 5 for future numerical comparisons. In addition, the load versus slip relations were also plotted in Fig. 6.

3. Elastic finite element analysis

The finite element program ANSYS was used to analyze the elastic rigidity of steel-concrete composite beams with full openings in the concrete flange. In the elastic analysis the materials were considered as elastic materials and the nonlinear property of material and geometry was not considered. Description of the FEA model is shown in Fig. 7(a). The elastic shell element was used to simulate the steel

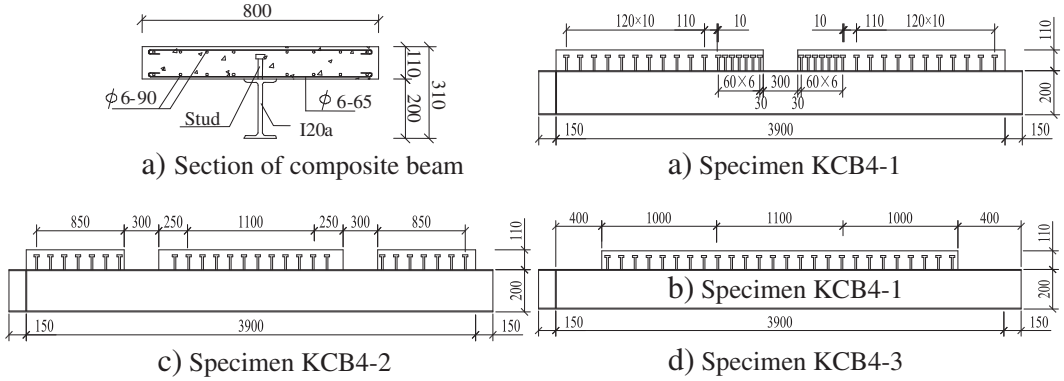

Fig. 2. Physical dimensions of specimens (unit = mm).

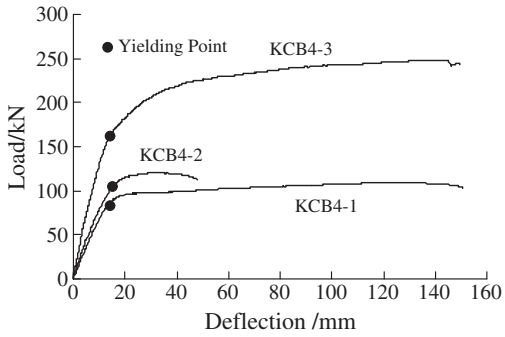

Fig. 4. Load–deflection curves of test specimens.

Table 1
Main results of test specimens (kN, mm).

Specimen	P_y	f_y	s_y	P_u	f_u	s_u	P_y/P_u	f_u/f_y
KCB4-1	77.7	11.06	0.004	109.3	118.5	0.072	0.71	10.7
KCB4-2	112.8	10.18	0.305	120.2	35.9	0.333	0.94	3.5
KCB4-3	171.3	12.86	0.837	248.5	141.6	8.5	0.69	11.0

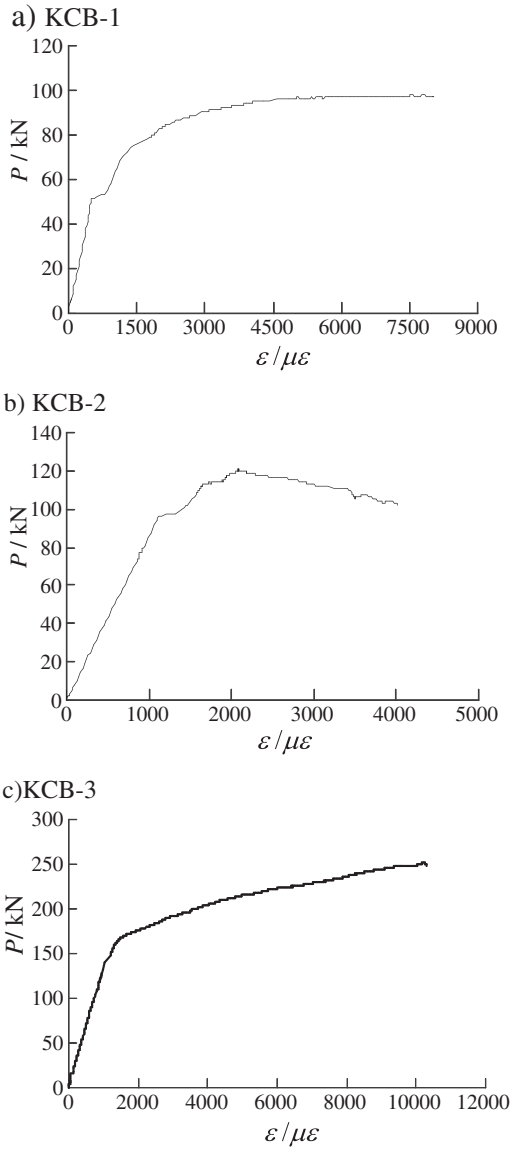

Fig. 5. Load–steel strain curves of test specimens.

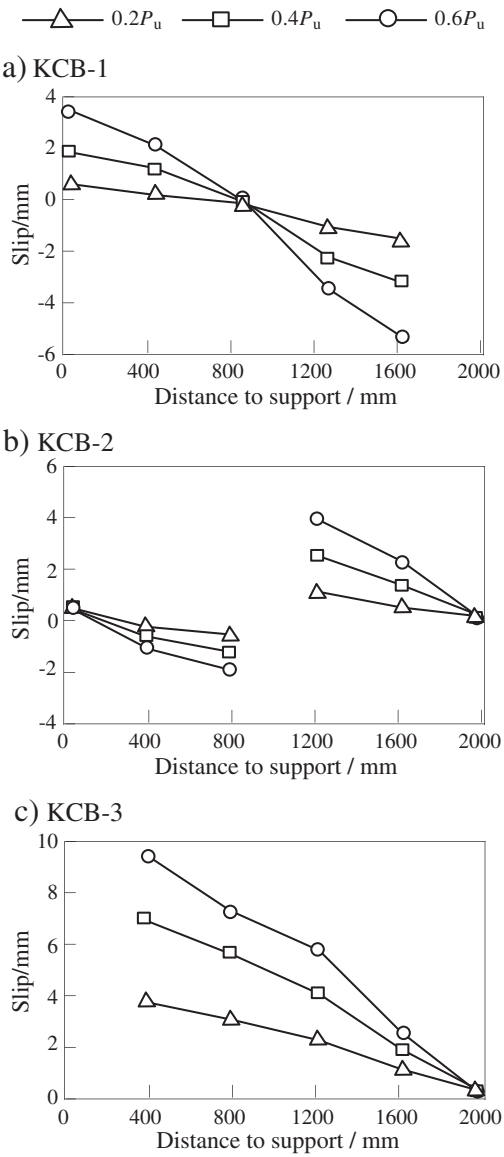

Fig. 6. Load–slip curves of test specimens.

beam and the elastic solid element was used to simulate the concrete slab. The steel bars in the concrete slab were ignored because they had little effect on the rigidity of beams in the elastic stage. The elastic modulus and Poisson's ratio were determined by experimental results and the experiential formulae [6]. The displacement constraint conditions were simple supported at the bearing and the load conditions were the same as the conditions used in experiments. The FEA models of the three specimens were shown in Fig. 8. There were two ways to establish the interface behavior of concrete and steel in the finite element model:

1) If the slips between the concrete and steel were not considered, the nodes in the interface of concrete and steel could be coupled in all degrees of freedom.
2) If the slips between the concrete and steel were considered, linear spring elements could be used to simulate the shear connectors between the concrete slab and steel beam as shown in Fig. 7(b). In the elastic stage, the slip usually existed only in the *X* direction and not in the *Y* direction due to the symmetrical characteristic about the *Z* axis. The separation of steel and concrete would not happen in the *Z* direction usually. Therefore, in the FEA model the two nodes B and B′ were connected with linear spring

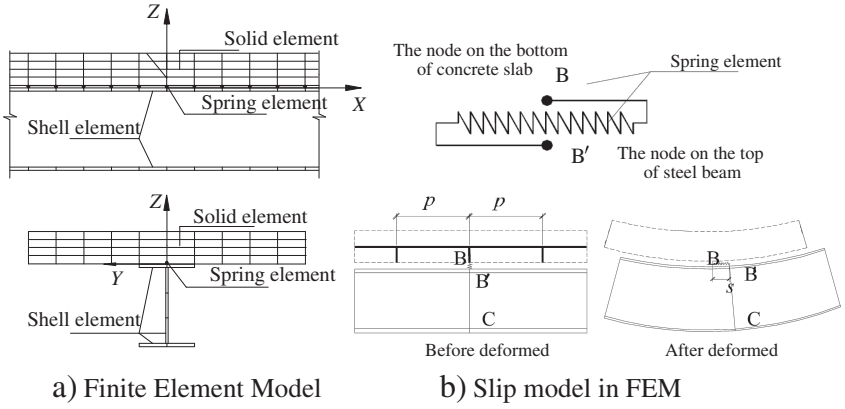

Fig. 7. Elastic finite element model of composite beam.

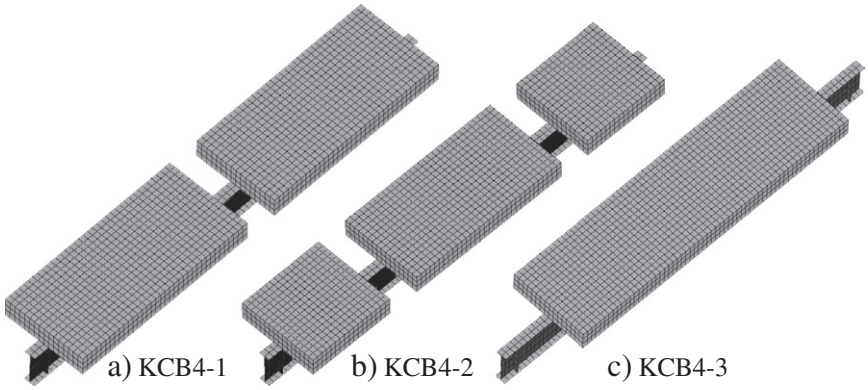

Fig. 8. Finite element model of test beams.

elements and coupled in the other two degrees of freedom except in the X direction. Before the beam deformed, the two nodes B and B′ were located at the same position. When the beam deformed, the slip happened in the X direction in the interface of the steel and concrete. The value of slip was BB′ as illustrated in Fig. 7(b). The stiffness of spring elements was K and the distance of the spring elements was p. Therefore, the shear stiffness of shear connectors per unit length in the interface of the steel and concrete was K/p. Supposing that the distance of shear connectors in the specimens was p', the shear bearing capacity of shear connectors was V_u and the number of shear connectors in the same section was n_s, the shear stiffness per unit length in the interface of steel and concrete k_s could be calculated as $0.66n_sV_u$ [7]. Making K/p in the FEA model equal to k_s could ensure the consistency between the FEA model (see Fig. 8) and the tests.

Table 2 showed that the deflection at the mid-span calculated by ANSYS was very close to the experimental results. Because the non-linear properties of concrete were not considered, the predicted deflection was slightly less than the experimental results. Fig. 9 showed the longitudinal distributions of the slip in the interface of concrete and steel. The FEA results were given alone due to the lack of sufficient measuring points. In the figure x was the distance from the mid-span to the section considered, l was the span length of specimens, and S_{max} was the maximum value of slip along the interface of the beams.

From Fig. 9 we can see that the distribution of the slip is much different between the composite beam with and without openings. For beams with openings, the maximum slip is not located at the end of the beam, but appears at the edge of openings, which has been verified by experiments. The slope of the slip curves is zero at the end of the beam, corresponding to the boundary condition of simply supported beams which is similar to the composite beam without openings.

The summation of longitudinal shear force caused by the studs must be zero because of the equilibrium condition of the axial force in the concrete slab. Because the shear force in the interface of the concrete and steel is proportion to the slip, the integration of the slip curve along the independent concrete slab should also be zero and this is then verified by checking the calculation.

4. Theoretical analysis

In order to analyze the elastic rigidity of steel-concrete composite beams with full openings in the concrete flange systematically, various load conditions and forms of openings were considered and shown in Fig. 10.

Based on the principle of superposition, the deflection at mid-span of steel-concrete composite beams with full openings can be separated into two parts:

$$f = f_e + \Delta f. \tag{1}$$

Table 2
Comparison of yielding defection between results of tests, FEA and theoretical method (mm).

Specimen	Load level	$f_{y,Test}$	$f_{y,FEA}$	$f_{y,FEA}/f_{y,Test}$	$f_{y,Theory}$	$f_{y,Theory}/f_{y,Test}$
KCB4-1	0.80 P_u	11.058	11.054	0.999	11.103	1.004
KCB4-2	0.65 P_u	10.177	9.895	0.972	9.711	0.954
KCB4-3	0.50 P_u	12.856	12.682	0.986	12.910	1.004

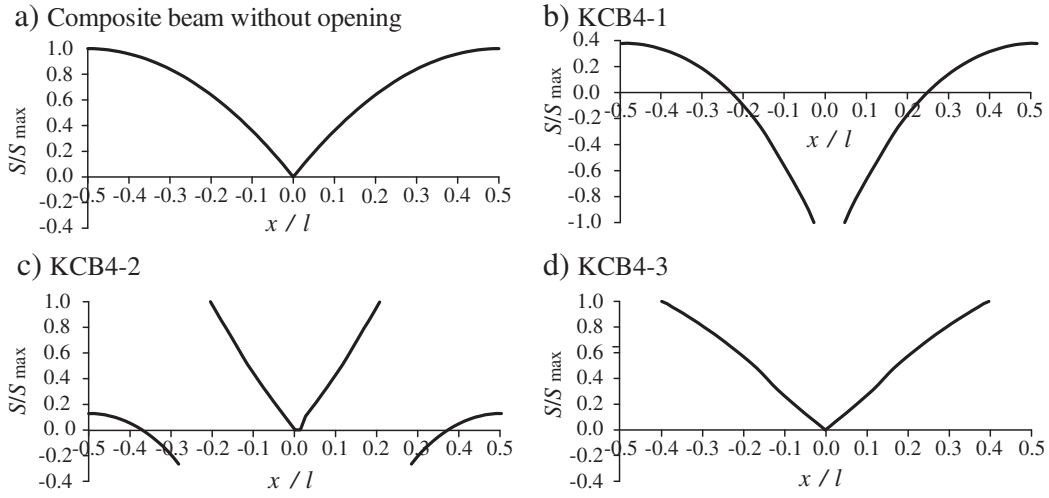

Fig. 9. Longitudinal distribution of slip between concrete and steel (2-point loaded).

Where f_e = the deflection at the mid-span calculated by transformed section method and Δf = the additional deflection at mid-span caused by the slip in the interface. The method to calculate the two parts of the deflection at mid-span will be developed separately in the next sections.

4.1. Deflection without considering slip

For the section at the edge of the openings, the normal stress caused by bending moment acts totally on the steel section, and no stress exists in the concrete section as shown in Fig. 11(a). From Saint-Venant's Principle [8] the normal stress gradually becomes uniform in the transverse direction. The inclination of compressive stress flow in the concrete slab at the edge of openings is defined in Fig. 11(a) as θ to the longitudinal axis. ANSYS was used to calculate the relationship between the values of tanθ and the width or height of the concrete slab. The θ can be found in FEM based on compressive stress trajectory of concrete slab in the stress nephogram. The results are listed in Table 3.

It can be seen from Table 3 that the value of tanθ is very close to 1.0. Therefore, the angle of the compressive stress flow approaches to 45°. In order to simplify the procedure of calculation, θ is assumed to be 45° in the present study. The concrete which is outside this dispersion angle has no contribution to the rigidity of the beams, as identified in the shadowed parts shown in Fig. 11(b).

Based on the transformed section method, the neutral axis of the composite section should be determined according to the axial force equilibrium on the section, neglecting the contribution to the section rigidity by the concrete below the neutral axis due to cracking. As a result, the second moment of area of the composite section near the openings considering the cracks of concrete can be calculated as:

$$I(z) = I_s + \frac{I_c(z)}{\alpha_E} + \frac{d_c^2 A_s A_c(z)}{\alpha_E A_s + A_c(z)}. \tag{2}$$

Where I_s = the moment of inertia of the steel section, A_s = the area of the steel section, I_c is the moment of inertia of the concrete section above the neutral axis, A_c = the area of the concrete section above the neutral axis (relevant to the distance to the edge of openings z, $z \le 0.5(b_c - b_1)$), d_c = the distance from the centroid of steel section to the centroid of concrete area above the neutral axis, and α_E ($= E/E_c$) = the elastic modulus ratio of the steel to the concrete.

Eq. (2) is not convenient for applications and can be simplified as follows:

$$I(z) = I_0 - \frac{4(I_0 - I_s)}{(b_c - b_1)^2}\left(z - \frac{b_c - b_1}{2}\right)^2. \tag{3}$$

Where I_0 = the moment of inertia of the composite section without openings calculated by transformed section method.

The deflection at mid-span of the composite beam is equal to the summation of the curvature-area taking moment about the support of all the infinitesimal segments of composite beams [9]. Therefore,

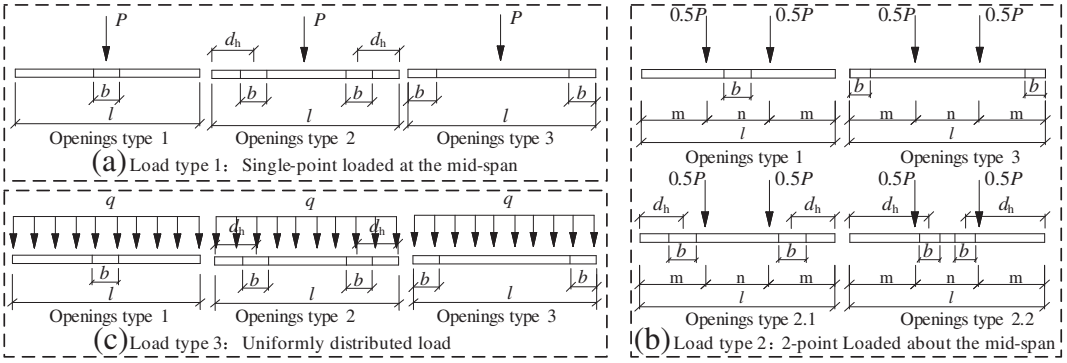

Fig. 10. Various forms of load and openings.

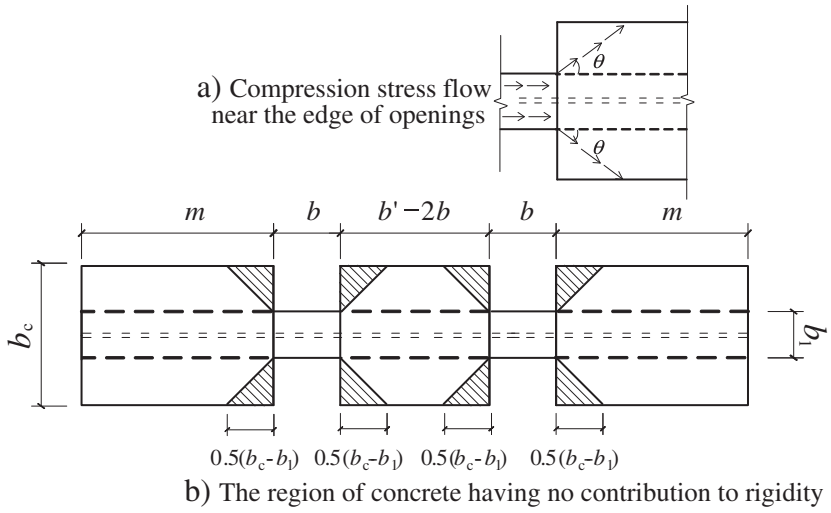

Fig. 11. Reduced rigidity near the edge of openings.

Eq. (3) can be introduced into Eq. (4) according to the equivalence of curvature-area as:

$$\int_0^{0.5(b_c-b_1)} \frac{Mdz}{EI(z)} = \frac{0.5(b_c-b_1)M}{EI_{eq}}. \quad (4)$$

Solving Eq. (4) leads to the equivalent moment of inertia of the section near openings as:

$$EI_{eq} = \eta EI_0 \quad (5)$$

Where

$$\eta = \frac{2\sqrt{1-k}}{\ln\left(\frac{2-k+2\sqrt{1-k}}{k}\right)}$$

and

$$k = I/I_0.$$

The beam model with variable stiffness along the beam shown in Fig. 12 can be used to calculate the deflection at mid-span based on the transformed section method with consideration of the effects of the non-uniform normal stress distribution at the edge of openings on the elastic rigidity.

Based on the curvature-area method [9], the formulas to calculate the deflection at the mid-span f_e using transformed section method are shown in Fig. 13 without showing the deriving process for the brevity of presentation, where d_h is the position of the openings defined as the distance from the center of the opening to the end of the beam.

In order to verify the accuracy of formulas in Fig. 13, comparisons are made between theoretical results and FEA results without consideration of slip effects by changing the width of the openings. The same parameters used are based on specimens in experiments. The point load is 80 kN and the uniform load is 13.3 kN/m. The results are plotted in Fig. 14 for comparison.

From Fig. 14 it is shown that the theoretical results and FEA results are very close so that the formulas in Fig. 13 can be reliably used to calculate the deflection at mid-span without considering the slip effect. Meanwhile, it is founded that openings near the supports have little effects on the deflection at mid-span. However, this effect becomes significant when the openings approach to the mid-span.

Table 3
Values of tanθ with various widths b_c and depths of concrete slab h_c.

h_c (mm)	b_c (mm)		
	800	1200	1600
100	0.98	0.94	0.90
150	0.99	0.93	0.91
200	1.01	0.98	.99

4.2. Additional deflection considering slip effects

Transformed section method is the basic method to calculate the rigidity of composite beams. Ref. [10] indicated that the rigidity of composite beams would be reduced by the effects of the slip in the interface of steel and concrete. Ref. [11] established the differential flexural formula considering the slip effects, but the formula could not be directly applied to obtain the additional deflection due to slip effects. Ref. [12] proposed a calculation method for the deflection of partial-connection composite beams, but the slip effects for full-connection composite beams were not considered.

At present there are mainly two methods to calculate the bending rigidity of the common composite beam considering the slip effects: (1) The effective moment of inertia method presented by refs. [13,14] adopted by AISC code. (2) The reduced rigidity method presented by ref. [7] and adopted by Chinese code [15]. A large number of references and research reports have shown that the rigidity calculated by the transformed section method and effective inertia method for partially composite beams is larger than the real rigidity, which leads to smaller deflections. In comparison, the reduced rigidity method can predict the rigidity more accurately and reflect the mechanical property sufficiently [16]. The AISC Commentary [13] also recommended using only 75% of the calculated effective inertia in order to obtain better results.

The slip distribution in composite beams with full openings is much different from common composite beams without openings. The slip still exists even in the pure bending zone of the beam and this is already verified in experimental research and FEA analysis. The reduced rigidity method is based on the differential equation of the interface of concrete and steel of composite beams without openings. Using the reduced rigidity method directly to calculate the rigidity of composite beams with full openings will cause the calculated rigidity larger than the real rigidity, and the mechanical property cannot be reflected properly. The openings can increase the slip and change the distribution pattern of the slip. Therefore, it is necessary to analyze the slip effects on the composite beam with

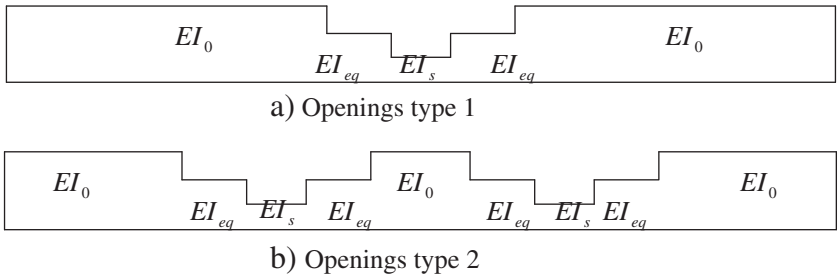

Fig. 12. Calculation model of deflection of transformed section.

full openings in the slab based on the basic principle of the reduced rigidity method.

The slip on the concrete slabs and steel beam should be discussed separately. As shown in Fig. 15, the concrete slabs are defined as two types: the one at side and the one in center. Fig. 15 shows the type 2 openings of composite beams. As for the types 1 and 3, it can be regarded as the beams with openings only at side or in center. Based on the deformed model of the composite beam in Fig. 16(a), the slip effects are discussed with various typical load conditions.

4.2.1. Single-point loaded at the mid-span

4.2.1.1. Additional deflection Δf_1 due to the side slip. Derivation of this part is the same as that conducted by ref. [16]. For the brevity of presentation, the derived differential equation for the slip displacement is given below directly:

$$S'' = \alpha^2 S - \frac{\alpha^2 \beta P}{2} \tag{6}$$

Where

$$\left(\alpha^2 = \frac{k_s A_1}{EI_0 p'},\ \beta = \frac{hp'}{2k_s A_1}, A_1 = \frac{I_0 + A_0 d_c^2}{A_0};\ A_0 \frac{A_c A_s}{\alpha_E A_s + A_c}\right).$$

After the differential equation of the slip in the interface is established, the boundary conditions of the differential equation should be given in order to solve the differential equation. The strain ε_{tb} and ε_{tt} is zero when $x = l/2$ because the moment at the end of the beam is zero. Therefore, the first boundary condition is obtained as $x = l/2$, $S' = 0$. Since the concrete section at the edge of openings does not share the moment and the moment is totally carried by the steel section, the tension strain on the concrete bottom ε_{tb} is zero and the compression strain on the steel top ε_{tt} is $-M_h(h_s - y_s)/E_s I_s$. Then the second boundary condition is obtained as: when $x = b''/2$,

$$S' = \varepsilon_{th} - \varepsilon_{tt} = \varepsilon_{tt} = \frac{M_h}{E_s I_s}(h_s - y_s). \tag{7}$$

Single point load at middle span : $f_e = \kappa P/48EI_0$

Type 1 $\kappa = (l - b + b_1 - b_c)^3 + [(l-b)^3 - (l - b + b_1 - b_c)^3]/\eta + [l^3 - (l-b)^3]/k$

Type 2 $\kappa = (2d_h - b + b_1 - b_c)^3 - (2d_h + b - b_1 + b_c)^3 + [(2d_h + b)^3 - (2d_h - b)^3]/k$
$+ [(2d_h - b)^3 - (2d_h - b + b_1 - b_c)^3 + (2d_h + b - b_1 + b_c)^3 - (2d_h + b)^3]/\eta + l^3$

Type 3 $\kappa = l^3 - 8b^3 + 8b^3/k$

2 point load about middle span : $f_e = \kappa P/12EI_0$

Type 1 $\kappa = 2m^3 + 3m(b_c - b_1)(2l - 2b - b_c + b_1)/4\eta + 3bm(2l - b)/4k + 3m(2m + l - b - b_c + b_1)(l - b - b_c + b_1 - 2m)/4$

Type 2.1 $\kappa = \{(2d_h - b + b_1 - b_c)^3 - (2d_h + b - b_1 + b_c)^3 + [(2d_h + b)^3 - (2d_h - b)^3]/k$
$+ [(2d_h - b)^3 - (2d_h - b + b_1 - b_c)^3 + (2d_h + b - b_1 + b_c)^3 - (2d_h + b)^3]/\eta + m^3 + 3m(l - 2m)(l + 2m)]\}/4$

Type 2.2 $\kappa = 2 + 6mbd_h/k + 6m(b_c - b_1)d_h/\eta + [3m(l + 2d_h + b + b_c - b_1)(l - 2d_h - b - b_c + b_1)$
$+ 3m(2d_h - b - b_c + b_1 - 2m)(2m + 2d_h - b - b_c + b_1)]/4$

Type 3 $\kappa = 2b^3/k - 2b^3 + 3ml^2/4 - m^3$

Uniformly distribute load : $f_e = \kappa q/48EI_0$

Type 1 $\kappa = l(l - b + b_1 - b_c)^3 + l[(l-b)^3 - (l - b + b_1 - b_c)^3]/\eta + l[l^3 - (l-b)^3]/k - 3\{(l - b + b_1 - b_c)^4$
$+ [(l-b)^4 - (l - b + b_1 - b_c)^4]/\eta + [l^4 - (l-b)^4]/k\}/8$

Type 2 $\kappa = \{[(2d_h - b + b_1 - b_c)^3 - (2d_h + b - b_1 + b_c)^3]l + [(2d_h + b)^3 - (2d_h - b)^3]l/k + [(2d_h - b)^3 - (2d_h - b + b_1 - b_c)^3$
$+ (2d_h + b - b_1 + b_c)^3 - (2d_h + b)^3]l/\eta + l^4\} - 3[(2d_h - b + b_1 - b_c)^4 - (2d_h + b - b_1 + b_c)^4 + [(2d_h + b)^4 - (2d_h - b)^4]/k$
$+ [(2d_h - b)^4 - (2d_h - b + b_1 - b_c)^4 + (2d_h + b - b_1 + b_c)^4 - (2d_h + b)^4]/\eta + l^4]/8$

Type 3 $\kappa = (l^4 - 8lb^3 + 8lb^3/k) - 3(l^4 - 16b^4 + 16b^4/k)/8$

Fig. 13. f_e calculated by transformed section method.

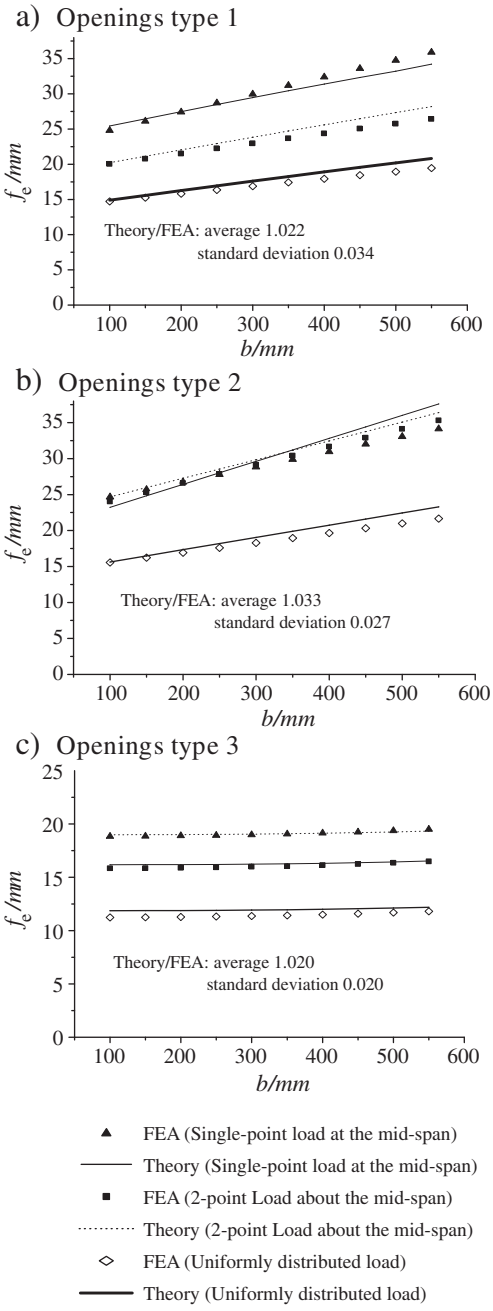

Fig. 14. Comparison between theoretical results and FEA results.

Where M_h = the moment at the edge of the openings. Define $\varepsilon_h = M_h(h_s - y_s)/E_s I_s$

Introducing the two boundary conditions into the differential equation, the equation can be solved as

$$S = \frac{\beta P}{2} + \left(\frac{e^{\alpha l-\alpha x} + e^{\alpha x}}{e^{\alpha l-\alpha b''/2} - e^{\alpha b''/2}}\right)\frac{\varepsilon_h}{\alpha}. \tag{8}$$

Differentiating Eq. (8), the slip strain is calculated as:

$$\varepsilon_s = S' = \left(\frac{e^{\alpha x} - e^{\alpha l-\alpha x}}{e^{\alpha l-\alpha b''/2} - e^{\alpha b''/2}}\right)\varepsilon_h. \tag{9}$$

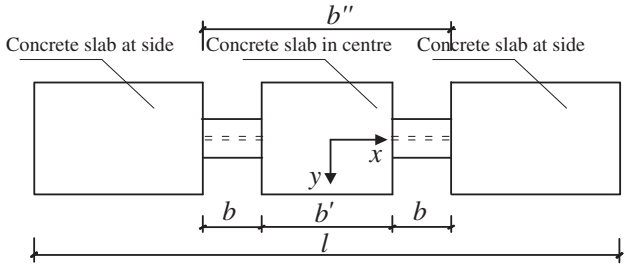

Fig. 15. Geometry parameter of concrete slab.

The strain distribution along the height direction of the composite section due to slip effects is shown in Fig. 16(b). Then the additional curvature can be calculated as:

$$\Delta\phi = \varepsilon_s/h. \tag{10}$$

Integrating the additional curvature along the beam the additional deflection at mid-span caused by effects of the slip in the interface of steel beam and concrete slab at side is calculated as:

$$\Delta f_1 = \int_{b''/2}^{l/2} \Delta\phi(l/2 - x)dx. \tag{11}$$

Solving the formulae above, the additional deflection is obtained as:

$$\Delta f_1 = \frac{(2-\alpha l + \alpha b'')e^{\alpha l} - (\alpha l - \alpha b'' + 2)e^{\alpha b''}}{2\alpha^2 h\left(e^{\alpha l} - e^{\alpha b''}\right)}\varepsilon_h. \tag{12}$$

4.2.1.2. Additional deflection Δf_2 due to the center slip. The differential equation of the slip in the interface is the same as Eq. (6). The first boundary condition is $x = 0, S = 0$ due to symmetry. The second boundary condition is when $x = b'/2$,

$$S' = \varepsilon_{tb} - \varepsilon_{tt} = \varepsilon_{tt} - \varepsilon_h. \tag{13}$$

Introducing the two boundary conditions into the differential equation, the differential equation is solved as:

$$S = \left(1 - \frac{e^{\alpha b'-\alpha x} + e^{\alpha x}}{1 + e^{\alpha b'}}\right)\frac{\beta P}{2} + \frac{e^{\alpha b'/2+\alpha x} - e^{\alpha b'/2-\alpha x}}{\alpha\left(1 + e^{\alpha b'}\right)}\varepsilon_h. \tag{14}$$

Differentiating Eq. (14), the slip strain is calculated as:

$$\varepsilon_s = S' = -\frac{-e^{\alpha b'-\alpha x} + e^{\alpha x}}{1 + e^{\alpha b'}}\frac{\alpha\beta P}{2} + \frac{e^{\alpha b'/2-\alpha x} + e^{\alpha b'/2-\alpha x}}{1 + e^{\alpha b'}}\varepsilon_h. \tag{15}$$

Dividing ε_s by h gives the additional curvature, and then the additional deflection at mid-span is obtained as

$$\Delta f_2 = \frac{\beta P\left[\alpha b' + 2 + (\alpha b' - 2)e^{\alpha b'}\right]}{4\alpha h\left(1 + e^{\alpha b'}\right)} + \frac{\left[(\alpha b' - \alpha l + 2) + (\alpha l = 2\alpha b' + 2)e^{\alpha b'} - 4e^{\alpha b'/2}\right]}{2\alpha^2 h(1 + e\alpha b')}\varepsilon_h. \tag{16}$$

As for the composite beam without openings ($M_h = 0$, $b' = l$), the additional deflection at mid-span is:

$$\Delta f_2 = \frac{\beta P\left[\left(\alpha l + e^{\alpha l}\right) + 2\left(1 - e^{\alpha l}\right)\right]}{4\alpha h\left(1 + e^{\alpha l}\right)}. \tag{17}$$

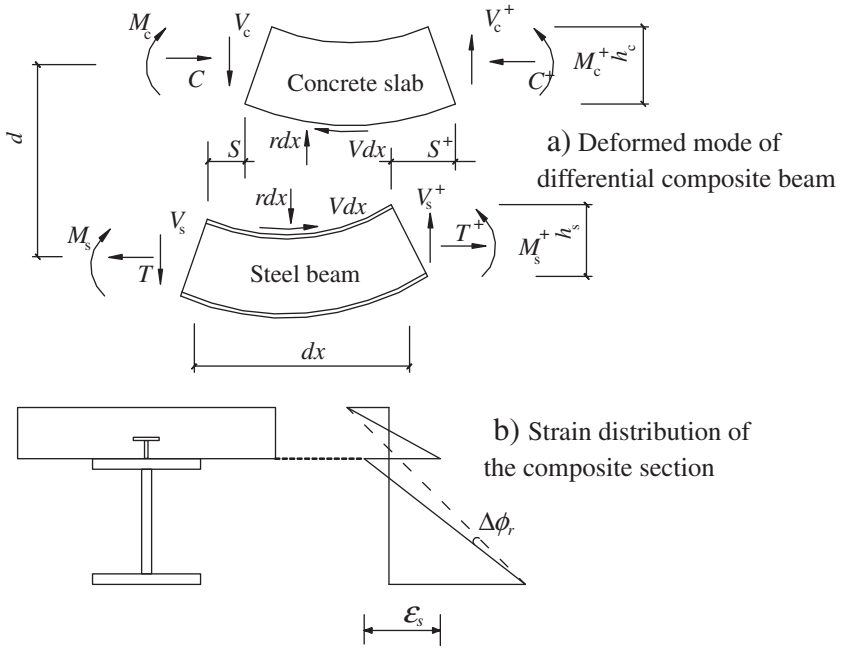

Fig. 16. Calculation model of composite beam considering slip.

In the same way the additional deflection at mid-span of composite beams with full openings under the load conditions of 2-point load about the mid-span and uniformly distributed load can be obtained. The detailed deriving process is ignored and the results are given below.

4.2.2. 2-Point loaded beam

4.2.2.1. Additional deflection Δf_1 due to the side slip.

$$\Delta f_2 = \frac{\beta P\left[m\alpha\left(1+e^{\alpha b'}\right)+e^{0.5\alpha b'-\alpha m}-e0.5^{\alpha b'+\alpha m}\right]}{2h\left(1+e^{\alpha b'}\right)} - \frac{\left[\left(\alpha b'-\alpha l+2\right)+\left(\alpha l-2\alpha b'+2\right)e^{\alpha b'}-4e^{\alpha b'/2}\right]\varepsilon_h}{2\alpha^2 h\left(1+e^{\alpha b'}\right)} \tag{18}$$

4.2.2.2. Additional deflection Δf_2 due to the center slip.

$$\Delta f_2 = -\frac{\left[\alpha b''-\alpha l-2+\left(\alpha b''-\alpha l+2\right)e^{\alpha l-\alpha b''}\right]\varepsilon_h}{2\alpha^2 h\left(e^{\alpha l-\alpha b''}+1\right)} \tag{19}$$

4.2.3. Uniformly distributed load

4.2.3.1. Additional deflection Δf_1 due to the side slip.

$$\Delta f_1 = \frac{\beta q b'^2}{8h} - \frac{\left(\varepsilon_h+\beta q\left[\left(\alpha b'-2\right)e^{\alpha b'}+4e^{\alpha b'/2}-\left(\alpha b'+2\right)\right]\right)}{2\alpha^2 h\left(1+e^{\alpha b'}\right)} \tag{20}$$

4.2.3.2. Additional deflection Δf_2 due to the center slip.

$$\Delta f_2 = \frac{\left(\begin{array}{l}\varepsilon_h-\beta q\left[2\alpha l e^{\frac{\alpha b''+\alpha l}{2}}-\alpha b'' e^{\alpha b''}-\left(\alpha b''+2\right)e^{\alpha l}\right] \\ +\beta q\left[\left(2\varepsilon_h+\alpha l\beta q\right)e^{\alpha b''}-\left(\alpha b''+2\right)e^{\frac{\alpha b''+\alpha l}{2}}\right]\end{array}\right)}{2\alpha^2 h\left(e^{\alpha l}-e^{\alpha b''}\right)} \tag{21}$$

The total deflection at mid-span is obtained once we know the additional deflection $\Delta f\ (=\Delta f_1+\Delta f_2)$ and the deflection f_e calculated by using the transformed section method. The comparison of test results and the results calculated by the proposed theoretical method is shown in Table 2. From the comparison we can see that the theoretical method is accurate enough to calculate the deflection at the mid-span of the steel-concrete composite beams with full openings in the concrete flange.

It is noted that for other boundary conditions such as in continuous beams rather than simply-supported beams, the calculation method for the additional deflection Δf is more complicated. We must confirm the boundary conditions at various positions along the beam, such as the section at the edge of openings, the section where the shear force is zero, the section where the moment is zero, and the section where the concentrated force exists. All the boundary conditions should be applied to solve the Newmark's differential equation and the slip equation can be obtained. By a piecewise integration of the additional curvature along the beam, the additional deflection caused by effects of the slip could be obtained.

5. Comparative analysis of elastic rigidity

In order to compare the accuracy of various methods, the calculated load–deflection curves in the elastic stage using various methods are plotted in Fig. 17, along with the measured results. Fig. 17 shows that without considering the openings or without considering the slip effect, the calculated deflection is smaller than the measured deflection. If we designed the composite beam with full openings as pure steel beam, the calculated deflection is much larger than the measured deflection, leading to a too conservative design. The calculated results are on the other hand unsafe by using the method developed for the composite beams with openings rates below 50% [5]. The FEA results and theoretical results from the present study both agree well with the experimental results. For specimen KCB4-3 that has openings near the supports, the calculated results are similar either considering or ignoring the openings. Therefore, it is verified that the openings near the supports have a small effect on the deflection at mid-span and this effect can be ignored.

6. Simplified method for calculation of elastic rigidity

The theoretical method presented in this paper is rather complicated and needs to be simplified for practical design. Considering the effects of the width and distance to the end of beam of openings b and d_h, the two non-dimensional parameters are defined as $\gamma = b/l$ and $\lambda = d_h/l$. Assume the equivalent rigidity can be expressed as

$$B_h = \frac{EI_0}{(1+\xi)(1+\xi_h)} \tag{22}$$

where ξ = the rigidity reduction factor for the slip effect developed by ref. [5] and ξ_h = the rigidity reduction factor considering effects of openings.

A large number of calculations were made to find the changing tendency of ξ_h versus parameters γ and λ. The results indicated that

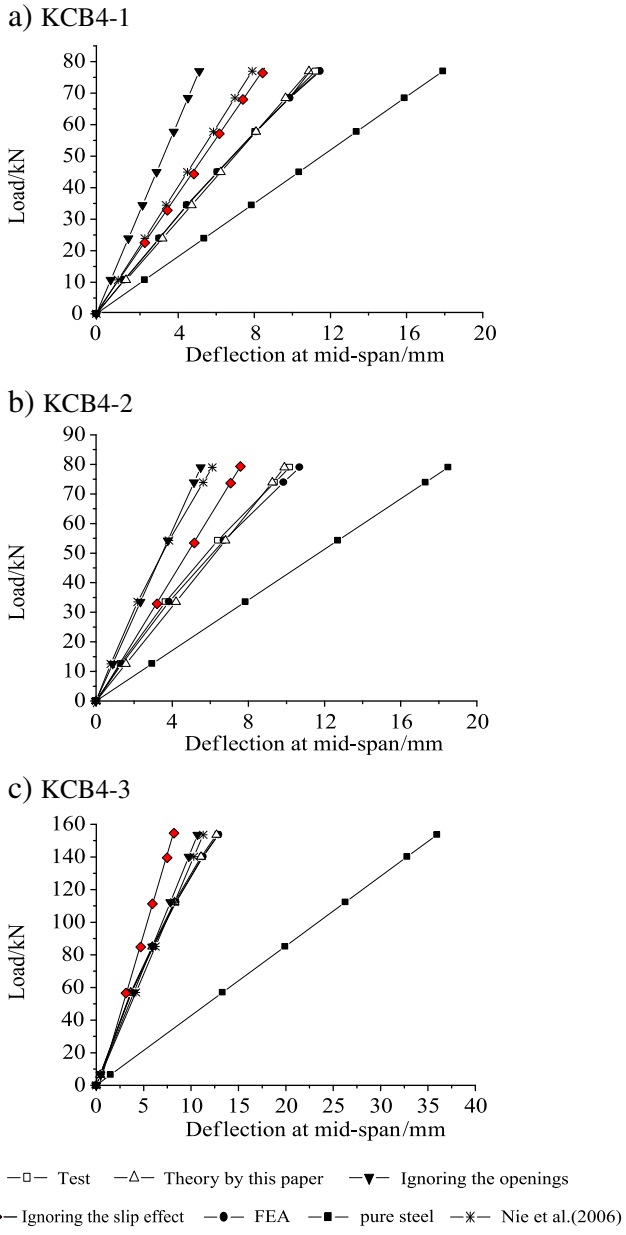

Fig. 17. Comparison of rigidity of test specimen used various methods.

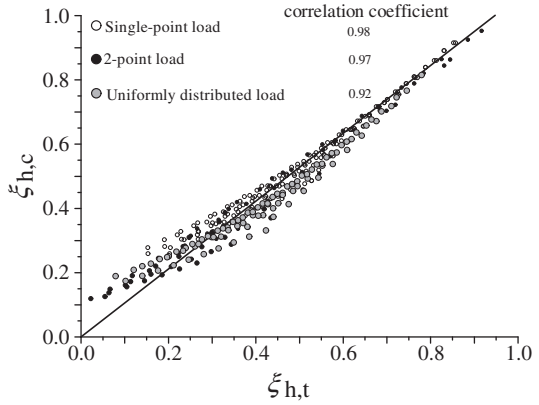

Fig. 18. Comparison of ξ_h between simplified method and theoretical method.

ξ_h is linear to γ and parabolic to λ. We can thus assume the expression of ξ_h as

$$\xi_h = a_1(\gamma + a_2)\left(\lambda^2 + a_3\lambda + a_4\right) \tag{23}$$

where a_1,a_2,a_3 and a_4 are the parameters to be determined.

Two-parameter non-linear regression is conducted to simplify the expression of ξ_h based on a large number of numerical calculations. The simplified expression of ξ_h is

$$\xi_h = \begin{cases} 230.43(\gamma - 0.0263)\left(\lambda^2 - 0.3165\lambda + 0.0311\right) \geq 0 & \text{(Single point load)} \\ 18.62(\gamma - 0.0289)\left(\lambda^2 + 0.6397\lambda + 0.0729\right) \geq 0 & \text{(2-point load)} \\ 8.53(\gamma - 0.0348)\left(\lambda^2 + 1.1529\lambda + 0.0701\right) \geq 0 & \text{(Uniform distributed load)} \end{cases} \tag{24}$$

It should be noted that Eq. (24) cannot satisfy the conditions without openings, namely when $\gamma = 0, \xi_h = 0$ and when $\lambda = 0, \xi_h = 0$. The main reasons are that the finite element model used to calculate the deflection of the composite beam with full openings in the concrete slab is not the same as the one used for regular composite beams without openings. As mentioned earlier, the stress flow in the concrete slab is not uniform in the transverse direction near the edge of openings and the moment at the edge of openings is carried by the pure steel section. There is great difference in the mechanical condition of the two types of composite beams. Therefore, Eq. (24) is not recommended for calculating the composite beam without openings.

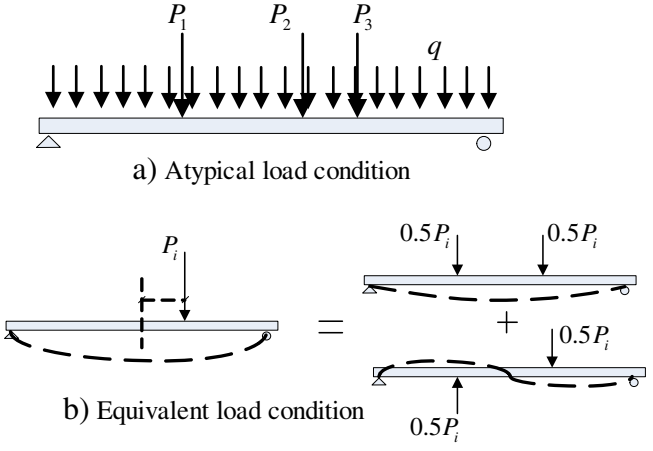

Fig. 19. Equivalent simplified method.

The values of ξ_h calculated by Eq. (24) ($\xi_{h,c}$) and theoretical method ($\xi_{h,t}$) are plotted by changing the two parameters γ and λ as shown in Fig. 18.

We can see from Fig. 18 that the simplified method is reliable to calculate the reduced rigidity factor considering openings. Therefore, we can regard the composite beam with full openings in the concrete flange as a beam with constant rigidity along the beam in design.

In practical design, the atypical load condition often exists as showed in Fig. 19(a). It is possible to decompose the atypical load condition to a uniformly distributed load condition and multiple single point load conditions. The deflection under the uniformly distributed load condition can be calculated by the simplified method proposed by this paper. Then the deflection under single point load conditions can be calculated by the equivalent simplified method as shown in Fig. 19(b). It can be seen from Fig. 19(b) that the asymmetrical single point load condition can be decomposed into symmetrical 2-point loaded condition and anti-symmetrical 2-point loaded condition. The deflection at mid-span under the former load condition can be calculated by the simplified method proposed by this paper, and the deflection at mid-span under the latter load condition is zero.

7. Conclusions

The FEA model developed in this paper can reliably predict the deflection of steel-concrete composite beams with full openings in the concrete flange. It can thus be used for the serviceability limit state design of steel-concrete composite beams with full openings in the concrete flange, which has been verified by comparison with test results.

The theoretical method is proposed to calculate the deflection of transformed section at mid-span with various forms of load and openings by appropriate assumptions. Then the formulae are derived for calculating the additional deflection at mid-span considering boundary conditions and the differential equation of slip between the concrete and steel interface. It is found that the theoretical results agree well with test results and it can be also used for the serviceability design of steel-concrete composite beams with full openings in the concrete flange.

The openings near the supports have small effects on the rigidity of steel-concrete composite beams with full openings in the concrete flange. This effect can thus be ignored when predicting the deflection at mid-span. As recommended by ref. [17], if the distance from the support to the openings is shorter than $L/8$, the effect of slab openings on the rigidity of composite beams could be safely ignored.

A simplified method is proposed by numerical regression for predicting the reduced rigidity of steel-concrete composite beams considering the slip and opening effects. The equivalent simplified method for atypical load conditions is also proposed. The simplified method is reasonable and convenient for application in practical design.

8. Notation

The following symbols are used in this paper:

A_s area of the steel section;
A_c area of the concrete section;
A_{st} area of the stud section;
a_1,a_2,a_3,a_4 regressed parameters;
b', b'' parameter determined by beam property;
B_h equivalent elastic rigidity of composite beam with full openings in concrete flange;
d_h position of the openings;
d_c distance from the centroid of steel section to the centroid of concrete section;
E elastic modulus of steel;
E_c elastic modulus of concrete;
f_e deflection without consideration of slip;
f_c compression strength of concrete;
f_u ultimate tension capacity of the stud;
f_y deflection when specimens yielding;
f_u deflection when specimens failure;
h_c height of concrete section;
h_s height of steel section;
h total height of composite beam;
I_c the moment of inertia of the concrete section;
I_0 moment of inertia of the composite section without openings calculated by transformed section method;
I_s moment of inertia of the steel section;
K stiffness of spring elements;
k_s shear stiffness per unit length in the interface of steel and concrete;
l span of specimens;
M_h moment at the edge of openings;
m,n parameter defined by 2-point load property;
n_s the number of shear connectors in the same section;
p' distance of shear connectors in specimens;
p distance of the spring elements;
P_u ultimate load of specimens;
P applied concentrated load;
P_y yielding load of specimens;
q applied uniformly distributed load;
s_y slip value when specimens yielding;
s_u slip value when specimens failure;
S_{max} maximum value of slip along the interface of the beams;
S slip at the interface of steel and concrete;
V_u shear bearing capacity of shear connectors;
z distance to the edge of openings;
α_E modulus ratio of the steel to the concrete;
α,A_1,A_0 parameter determined by beam section and material property;
η, k, parameter determined by beam section property;
θ Inclination of compressive stress flow in the concrete slab at the edge of openings;
Δf total additional deflection with consideration of slip;
Δf_1 additional deflection due to the side slip;
Δf_2 additional deflection due to the center slip;
$\Delta\phi$ additional curvature;
ϕ curvature of beam;
ε_{tb} tension strain on the concrete bottom;
ε_{tt} compression strain on the steel top;
ε_s slip strain at the interface of steel and concrete;
γ,λ parameter defined by openings property;
ξ_h rigidity reduction factor considering the effects of openings;
ξ rigidity reduction factor for slip effect.

Acknowledgments

The writers gratefully acknowledge the financial support provided by the National Outstanding Youth Fund of NFSC (50025822) and National Neutral Science Foundation of China (50438020 and 50828803).

References

[1] Nie JG, Yu ZW. Research and practice of composite steel-concrete beams in China. China Civ Eng J 1999;32(2):3–8.
[2] Benitez MA, Darwin D, Donahey RC. Deflection of composite beams with web openings. J Struct Eng 1998;124(10):1139–47.
[3] Ramm W, Kohlmeyer C. Shear-bearing capacity of the concrete slab at web openings in composite beams. Proceedings of the 5th International Conference on Composite Construction in Steel and Concrete; 2006. p. 214–25.

[4] Redwood RG, Poumbouras G. Tests of composite beams with web holes. Can J Civ Eng 1983;10(4):713–21.
[5] Nie JG, Cai CS, Wu H, Fan JS. Experimental and theoretical study of steel-concrete composite beams with openings in concrete flange. Eng Struct 2006;28(7): 992–1000.
[6] Kuranovas A, Goode D, Kvedaras AK, Zhong ST. Load-bearing capacity of concrete-filled steel columns. J Civ Eng Manage 2009;15(1):21–33.
[7] Nie JG, Shen JM, Yu ZW. A reduced rigidity method for calculating deformation of compo site steel-concrete beams. China Civ Eng J 1995;30(2):13–9.
[8] Sternberg E. On Saint-Venant's principle. Q Appl Math 1954;11(4):393–402.
[9] Timoshenko S, Gael J. Material mechanism. Beijing: Science Press; 1978.
[10] Johnson RP. Composite structures of steel and concrete, Vol. 1. Granada Publishing Limited; 1975.
[11] Newmark NM, Siess CP, Viest IM. Tests and analysis of composite beams with incomplete interaction. Exp Stress Anal 1951;9(1).
[12] Johnson RP, May IM. Partial-interaction design of composite beams 1975. Struct Eng 1975;53(8).
[13] AISC. Load and resistance factor design specification for structural steel buildings, IL, Chicago; 2010.
[14] Grant JA, Fisher JW, Slutter RG. Composite beams with formed steel deck. AISC Eng J 1977;12(1):24–43.
[15] GB 50017-2003. Code for design of steel structures. Beijing, China; 2003.
[16] Nie JG, Cai CS. Steel-concrete composite beams considering shear slip effect. J Struct Eng 2003;129(4):495–506.
[17] Kenneth B, Wiesner PE. Composite beams with slab openings. Mod Steel Constr March 1996:26–30.